

Influence of Carbon on the Wear Resistance, Strength, and Hardness of Composites with a Fe–Cr–Mn–Mo–N–C Matrix

M. S. Konovalov^{a,*}, V. I. Lad'yanov^a, M. I. Mokrushina^a, and P. G. Ovcharenko^a

^a*Udmurt Federal Research Center, Ural Division, Russian Academy of Sciences, Izhevsk, 426067 Russia*

**e-mail: maksim.kov@mail.ru*

Received January 20, 2023; revised February 10, 2023; accepted February 10, 2023

Abstract—Ingots of a composite with a Fe–Cr–Mn–Mo–N–C matrix and reinforcing particles in the form of MgO, Al₂O₃, and AlN conglomerates have been produced by aluminothermy, which is a version of self-propagating high-temperature synthesis (SHS). The ingots differed mainly in carbon content. It has been found that with an increase in carbon content in the composite from 0.01 to 0.50 wt %, its hardness rises from 238 to 271 HV and its wear resistance improves. The wear resistance has been estimated by abrasive testing under the conditions of dry friction between the sample and a fixed abrasive—electrocorundum P400 grit (28–40 μm) and P80 grit (200–250 μm) abrasive paper. As a measure of wear resistance, we chose a decrease in sample weight after tests. The pressure with which the test material acted on the abrasive was roughly equal to 0.25 N/mm², and the test time was 90 s. The loss in weight was been measured using VLR-200 balance. The hardness has been measured by Vickers hardness testing using an ITV-1-A hardness meter according to State Standard 2999-75 with a holding time of 10 s under a load of 30 kgf. It has been found that a rise in carbon content in the composite causes its embrittlement. It is noteworthy that in passing compressive strength tests samples with 0.01 and 0.16 wt % C remained intact, whereas those with 0.50 wt % C cracked. However, cracked samples continued deforming without complete breakdown up to a load that is maximum permissible for the test machine. The compressive strength has been estimated from the cracking load and has been found to be 3210 MPa. The ultimate compressive strength has been determined using an REM-100-A-2 multipurpose testing machine.

Keywords: composite, alloy, wear resistance, strength, hardness of composite, ultimate compressive strength

DOI: 10.1134/S1063784224700257

INTRODUCTION

In order to reach a high mechanical performance of corrosion-resistant steels, it seems promising to devise compositions providing joint doping with nitrogen and carbon [1]. In austenite, these elements form an interstitial solid solution stabilizing the alloy and improving its strength characteristics [1, 2]. Moreover, these elements improve the resistance of steels against specific types of corrosion, e.g., pitting corrosion [3], which is indirectly confirmed by the MARC index [3–6]. It was noted [4] that the combination of carbon and nitrogen may contribute to corrosion resistance and that of nickel and manganese has a detrimental effect.

Composite steels with a Fe–Cr–Mn–Mo–N–C matrix and reinforcing particles in the form of Al₂O₃, MgO, and AlN conglomerates are of interest as promising antifrictional materials. Their structure consisting of a mild matrix (alloyed steel) with uniformly embedded harder inclusions of conglomerates, in which magnesium oxide with aluminum oxide impurities is surrounded by aluminum nitride, is among the basic structures of metallic materials used in slide bearings. Most widely used metallic antifrictional

materials with a mild matrix and harder reinforcing inclusions are exemplified by babbitts [7–9]. However, these alloys are expensive and a trend is observed to replace them by cheaper materials. Specifically, composites with a Fe–Cr–Mn–Mo–N–C matrix and reinforcing particles in the form of Al₂O₃, MgO, and AlN conglomerates are viewed as an alternative.

Based on [10–12] it can be argued that SHS proceeding under a nitrogen pressure (a version of aluminothermy) is a highly cost-effective method to produce sparingly alloyed nickel-free high-nitrogen steels. Synthesis is usually carried out in special reactors, such as RVS-10. This reactor is schematically shown in Fig. 1 [10].

Melt carbonization in a reaction crucible (Fig. 1) is undesirable for the aluminometric process, since carbon becomes a stronger reducing agent at a temperature of this process (above 2273 K) according to the Ellingham diagram [13]. Consequently, with carbonizing agents added to the aluminothermic reaction mixture, the process will be accompanied by the uncontrollable and hardly predictable carbon-assisted reduction of resulting aluminum oxides, as well as

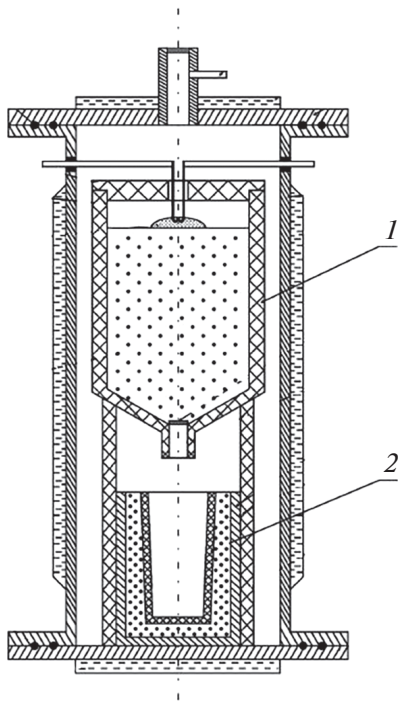


Fig. 1. Schematic of the RVS-10 reactor [10]: (1) reaction crucible and (2) cooling crucible.

chromium, molybdenum, and manganese oxides present in the reaction mixture. This leads to extremely high losses of alloying carbon and an excess of aluminum in the synthesized ingot and raises the risk of gas porosity.

After the burning front passing through the charge mixture reaches the diaphragm, it melts and the metal-slag melt flows out of the reaction crucible into the cooling one. Due to heat transfer, the products of the exothermal process that fell into the cooling crucible have a lower temperature than the temperature in the reaction crucible. Therefore, carbon alloying of composites with a Fe-Cr-Mn-Mo-N-C matrix and reinforcing particles in the form of Al_2O_3 , MgO, and AlN conglomerates obtained by aluminothermy in the cooling crucible seems to be the most useful way of melt carbonization (Fig. 1). Because of specific reactor designs, cooling crucibles often are not equipped with a forced heating system. In this case, the degree of carbonization is limited by the carbonizer dissolution time when the melt is kept in the interval between final synthesis temperature T_f and liquidus temperature T_l , which depends on the chemical composition of steel [14, 15]. Temperature T_l varies with the degree of carbon dissolution according to known relationships (see, e.g., [16, 17]). It was noted [14] that the diffusion and mechanical stirring of particles in melt are today the least understood processes in the dissolution theory.

Thus, the analysis and prediction of carbonization in melt cooling crucibles, as applied to Fe-Cr-Mn-Mo-N-C composites (including those containing Al_2O_3 , MgO, and AlN conglomerates) obtained in the aluminothermic process, are challenging problems that require taking account of many factors some of which are imperfectly known. Therefore, the development of carbon alloying technologies for the aluminothermy of the given composites should be aimed at improving their operational properties. For slide bearing materials, ultimate compressive strength, wear resistance, and hardness are such properties. However, for composites with a Fe-Cr-Mn-Mo-N-C matrix and reinforcing particles in the form of Al_2O_3 , MgO, and AlN conglomerates, relevant literature data that allow the estimation of carbon content influence on the above parameters are virtually absent.

The goal of this study was to estimate the influence of carbon content on the ultimate compressive strength, abrasive wear resistance, and hardness of composites with a Fe-Cr-Mn-Mo-N-C matrix and reinforcing particles in the form of Al_2O_3 , MgO, and AlN conglomerates.

MATERIALS AND INVESTIGATION TECHNIQUES

To carry out SHS in the aluminothermic process under nitrogen pressure, we used the following reagents: analytically pure Fe_2O_3 powder (specs 6-09-5346-87), OKhM-0 Cr_2O_3 powder (State Standard 2912-79), analytically pure MnO_2 powder (State Standard 4470-79), Ch TU 6-09-4471-77 MoO_3 powder, PAM-4 Al-Mg powder (State Standard 5593-78), ASD-1 aluminum powder (specs. 1791-99-019-98), and chromium nitrides obtained by nitriding PKh-1M chromium (specs. 14-1-1474-75) using SHS. To remove moisture and increase the specific surface area, oxides in the mixture were predried in an electrical furnace at 250°C for 1–2 h and grinded in a ball mill. The weighed components of the charge were processed in a mixer. The aluminothermic synthesis of high-nitrogen steels was carried out in an RVS-10 SHS reactor under a nitrogen pressure of up to 15 MPa (the burning-initiating nitrogen pressure was equal to 10 MPa and then, during burning, was increased to 15 MPa). The calculation of charge components and the selection of parameters for high-nitrogen steel synthesis with the aim of providing aluminum nitride in resulting ingots were made with allowance for process features mentioned in [11, 12].

Test samples were cut out of ingots by the electrical discharge method. The metal was studied after thermal treatment (aging at 1250°C for 2 h with subsequent water quenching).

A gas analysis to determine the nitrogen and oxygen concentrations was performed with a METAVAK-VAK analyzer by reduction melting in a carrier gas flow. The

Table 1. Chemical compositions of synthesized ingots, wt %

No.	Fe	Cr	Mn	Mo	Al	Mg	N	C	O
1	Base material	13.02	9.37	3.75	0.92	0.16	0.96	0.01	0.197
2	Base material	12.71	9.09	3.84	0.93	0.15	0.92	0.16	0.219
3	Base material	12.50	9.30	3.70	0.91	0.18	0.90	0.50	0.204

nitrogen concentration was detected with a thermal conductivity cell, and the oxygen concentration was determined from IR absorption data. The carbon content was found using a METAVAK CS-30 analyzer by

applying the burning test in an oxygen flow and recording resulting carbon dioxide by a detector.

A chemical analysis for metals was conducted on a Spectroflame Modula S inductively coupled plasma

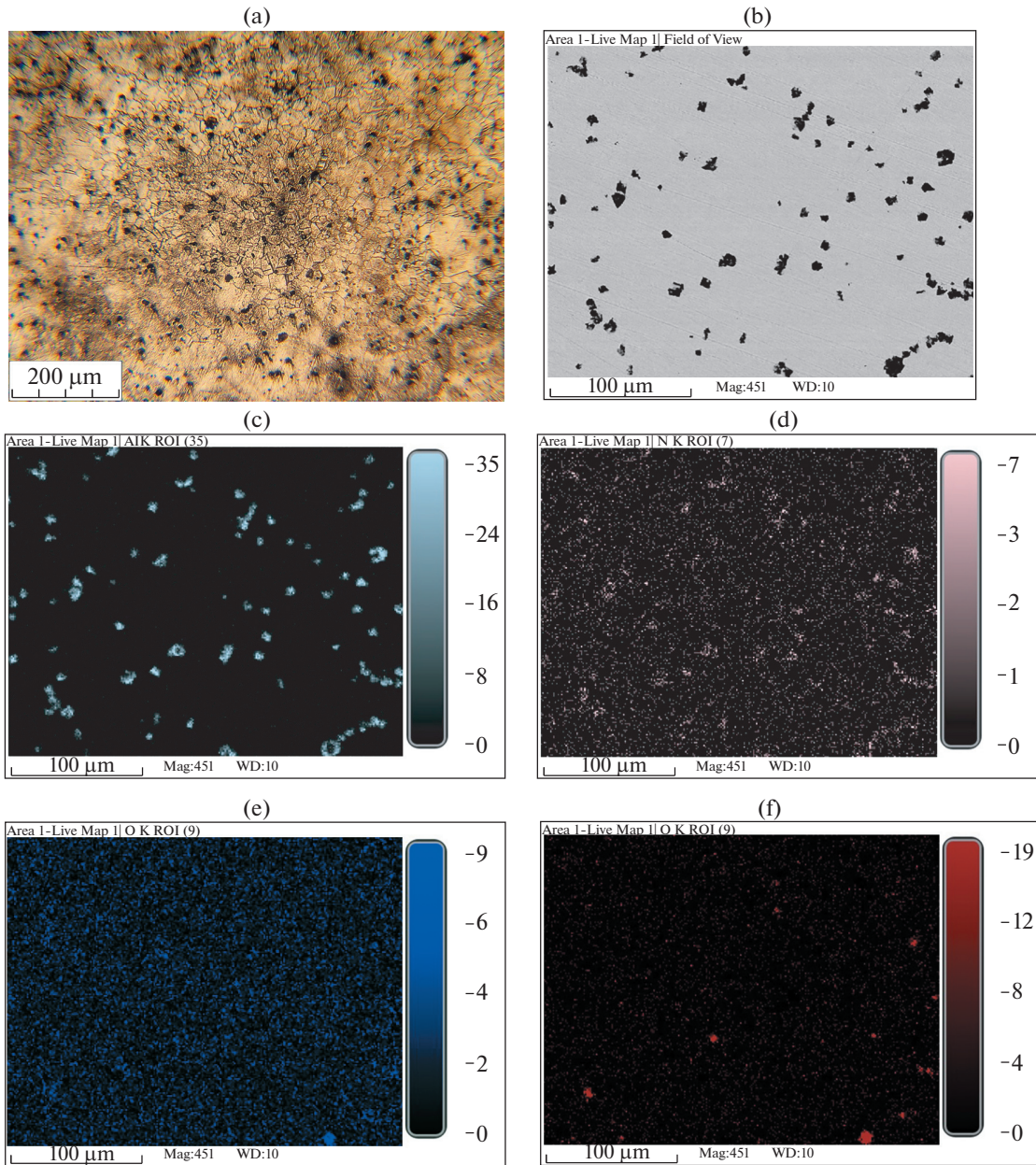


Fig. 2. (a) Metallographic and (b) electron microscopy data and concentration maps (a size scale of 100 μm) for (c) aluminum, (d) nitrogen, (e) oxygen, and (f) magnesium.

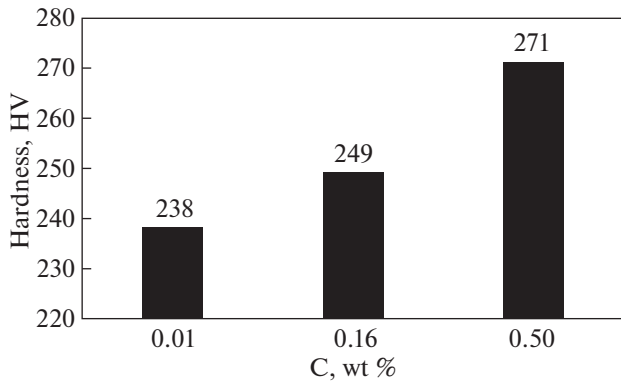


Fig. 3. Hardness test results.

atomic emission spectrometer, which provides high stability and high reliability of analysis data in a wide range of concentrations (including difficult-to-detect elements) [18, 19], and on a BRA-135F X-ray fluorescent energy-dispersive analyzer equipped with a KEDA-E software suite.

For metallographic examination, we used a NEOPHOT-21 microscope, and electron microscopic studies were performed with a Thermo Fisher Scientific Quattro S scanning electron microscope. The latter was equipped with a field emission gun and a system for energy-dispersive microanalysis based on an EDAX Octane Elect Plus EDS spectrometer.

Wear resistance tests were carried out under the conditions of dry friction on the surface of a fixed abrasive—electrocorundum P400 grit (28–40 μm) and P80 grit (200–250 μm) abrasive paper. As a measure of wear resistance, we used a decrease in sample weight after tests. The pressure with which the test material acted on the abrasive was roughly equal to 0.25 N/mm², and the test time was 90 s. The loss in weight was measured using VLR-200 balance.

Hardness measurements were carried out by the Vickers method using an ITV-1-A hardness tester in accordance with GOST 2999-75 with a holding time of 10 s at a load of 30 kgf.

RESULTS AND DISCUSSION

We synthesized three ingots with chemical compositions shown in Table 1. Each ingot was cut into pieces, which were then subjected to heat treatment. From these pieces, test samples were prepared.

Metallographic (Fig. 2a) and electron microscopic (Fig. 2b) data, as well as data of energy-dispersive analysis (Figs. 2c–2f), show that all heat-treated samples have the same structure. The composite has an austenite Fe–Cr–Mn–Mo–N–C matrix in which reinforcing particles (from 5 to 15 μm in size) uniformly extended in three directions are distributed. In concentration maps (Figs. 2c–2f) it is seen that some

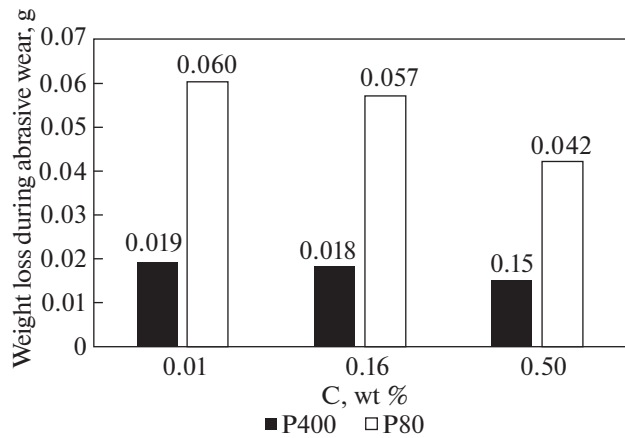


Fig. 4. Results of wear resistance comparative tests.

of conglomerates are “opened.” The center of these inclusions is occupied by MgO oxide with Al₂O₃ impurities, which is peripherally surrounded by AlN.

Hardness measurements demonstrate that the resistance of synthesized alloys against indenter penetration rises with carbon content in the matrix. Figure 3 plots the hardness of samples versus carbon content in them.

Data for abrasive-wear-induced weight loss (Fig. 4) indicate that the wear resistance of the composite alloy rises with carbon content in the matrix. In tests with P80 grit abrasive paper, the improvement of abrasive wear resistance is stronger than in the case of P400 paper. However, this effect is variable: when the carbon content increases from 0.01 to 0.06 wt %, the weight loss decreases by 5.0% in tests with P80 abra-

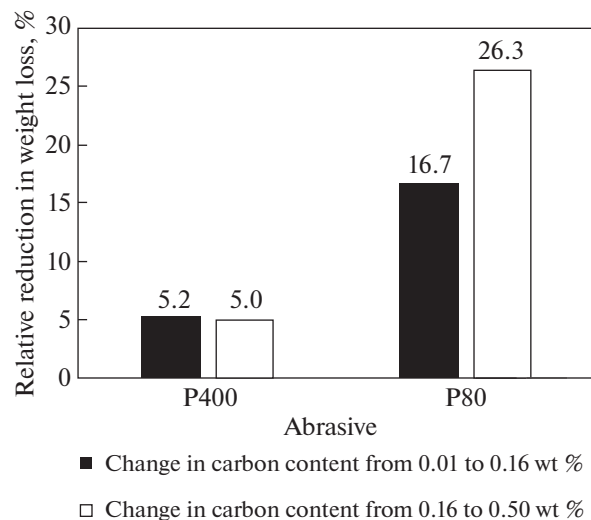


Fig. 5. Variation of the relative decrease in weight loss with increasing carbon content for two abrasives used in tests.



Fig. 6. Sample cracked after compressive strength test.

sive paper and by 5.2% in the case of P400 abrasive paper.

As the carbon content grows from 0.16 to 0.50 wt %, the weight loss drops by 26.3% in the case of P80 grit abrasive paper and by 16.7% in the case of P400 grit paper. Figure 5 plots the variation of the relative decrease in weight loss with increasing carbon content for two abrasives used in tests.

Seemingly, the above effect is due to the fact that the grit size of P400 abrasive paper (28–40 μm) is closer to the size of reinforcing particles (5–15 μm) than that of P80 paper (200–250 μm). It therefore appears that the matrix has a greater influence on the wear resistance measured in tests with P80 abrasive paper than on the wear resistance obtained in tests with P400 one. In addition, the variation of sample weight loss suggests that reinforcing particles are tightly bound to the matrix: no enhanced pitting is observed at abrasive wear.

After tests for ultimate compressive strength, samples containing 0.01 and 0.16 wt % C remained intact. Those with 0.50 wt % C cracked but continued deforming without complete breakdown up to a load that is maximum permissible for the test machine. The compressive strength of the composite with 0.50 wt % C was equal to 3210 MPa, as determined from the cracking load. The sample cracked after tests is shown in Fig. 6.

The above results indicate that the compressive strength of the composite with 0.50 wt % C is close to the ultimate compressive strength of wear-resistant cast iron with 17.5 wt % Cr, 1.5 wt % Mo, 1.0 wt % Cu, and 3.0 wt % C (3270 MPa), which was quenched from 1010°C and used for reference.

The integrity of samples with 0.01 and 0.16 wt % C after tests for ultimate compressive strength and the formation of cracks in the sample with 0.50 wt % C, which yet continued deforming without complete

breakdown up to a load that is maximum permissible for the testing machine, indicate very tight bonding between reinforcing particles and composite's matrix. The increase in carbon content to 0.50 wt % causes the embrittlement of the composite. Thus, further increasing the concentration of carbon dissolved in the matrix seems unreasonable.

CONCLUSIONS

(i) It was found that the increase in carbon content from 0.01 to 0.50 wt % in a composite with a Fe–Cr–Mn–Mo–N–C matrix and reinforcing particles in the form of MgO, Al₂O₃, and AlN conglomerates raises its hardness from 238 to 271 HV.

(ii) The increase in carbon content in the composite from 0.01 to 0.50 wt % improves its abrasive wear resistance.

(iii) The increase in carbon content in the composite from 0.01 to 0.50 wt % causes its embrittlement (in tests for compressive strength, samples with 0.01 and 0.16 wt % C remained intact and those with 0.50 wt % cracked). The ultimate compressive strength was found to be 3210 MPa.

ACKNOWLEDGEMENTS

The authors thank V.A. Karev for ingot synthesis and I.K. Averkiev for conducting electron microscopic examination and energy-dispersive analysis.

FUNDING

This study was carried out in the framework of research project no. 121030100001-3 using equipment in the Center for Collective Use at the Udmurt Federal Research Center, Ural Division, Russian Academy of Sciences.

CONFLICT OF INTEREST

The authors declare that they have no conflicts of interest.

REFERENCES

1. A. G. Svyazhin and L. M. Kaputkina, *Izv. Vyssh. Uchebn. Zaved., Chern. Metall.* **62** (3), 173 (2019). <https://doi.org/10.17073/0368-0797-2019-3-173-187>
2. M. V. Kostina and L. G. Rigina, *Izv. Vyssh. Uchebn. Zaved., Chern. Metall.* **63** (3), 606 (2020). <https://doi.org/10.17073/0368-0797-2020-8-606-622>
3. A. N. Maznichevskii, Yu. N. Goikhenberg, and R. V. Sprikut, *Vestn. Yuzhno-Ural'sk. Gos. Univ. Ser. Metall.* **20** (3), 42 (2020). <https://doi.org/10.14529/met200305>
4. M. O. Speidel, *Materialwiss. Werkstofftech.* **37** (10), 875 (2006). <https://doi.org/10.1002/mawe.200600068>

5. M. O. Speidel, *Met. Sci. Heat Treat.* **47** (11–12), 489 (2005).
<https://doi.org/10.1007/s11041-006-0017-y>
6. E. A. Merkushin and V. V. Berezovskaya, *Vestn. Tambovsk. Univ. Ser. Estestv. Tekh. Nauki* **21** (3), 1160 (2016).
<https://doi.org/10.20310/1810-0198-2016-21-3-1160-1163>
7. L. G. Korshunov, N. I. Noskova, A. V. Korznikov, N. L. Chernenko, and N. F. Vil'danova, *Phys. Met. Metallogr.* **108** (5), 519 (2009).
<https://doi.org/10.1134/S0031918X0911012X>
8. V. V. Ilyushin and B. A. Potekhin, *Lit'e Metall.*, No. 3S (57), 69 (2010).
<https://doi.org/10.21122/1683-6065-2010-3-69-72>
9. I. E. Kalashnikov, L. K. Bolotova, L. I. Kobeleva, I. V. Katin, P. A. Bykov, A. G. Kolmakov, R. S. Mikheev, and N. V. Kobernik, RF Patent No. 2585588 (2016).
10. G. Dorofeev, V. Karev, O. Goncharov, E. Kuzminykh, I. Sapegina, A. Lubnin, M. Mokrushina, and V. Lad'yanov, *Metall. Mater. Trans. B* **50** (2), 632 (2019).
<https://doi.org/10.1007/s11663-018-1499-x>
11. V. I. Lad'yanov, G. A. Dorofeev, E. V. Kuz'minykh, V. A. Karev, and A. N. Lubnin, *Izv. Vyssh. Uchebn. Zaved., Chern. Metall.* **62** (2), 154 (2019).
<https://doi.org/10.17073/0368-0797-2019-2-154-162>
12. G. A. Dorofeev, V. A. Karev, E. V. Kuzminykh, V. I. Lad'yanov, A. N. Lubnin, A. S. Vaulin, and M. I. Mokrushina, *Russ. Metall. (Metally)* **2013** (1), 1 (2013).
<https://doi.org/10.1134/S0036029513010047>
13. A. Yu. Zuev and D. S. Tsvetkov, *Chemical Thermodynamics: Textbook* (Ural Univ., Yekaterinburg, 2020) [in Russian].
14. V. F. Sobolev, N. V. Andriyanov, and A. A. Chichko, *Lit'e Metall.*, No. 4 (32), 72 (2004). <https://www.elibrary.ru/item.asp?id=50149824>.
15. M. L. Lobanov and M. A. Zorina, *Methods for determining diffusion coefficients: A tutorial*, (Ural Univ., Yekaterinburg, 2017) [in Russian].
16. S. M. Kabishov, I. A. Trusova, P. Je. Ratnikov, and S. V. Korneev, *Litiyo i Metallurgiya* **79** (2), 82, 2015 [in Russian].
17. L. A. Smirnov, A. G. Gudov, S. P. Burmasov, A. S. Oryshchenko, and G. Yu. Kalinin, *Steel in Translation* **50** (10), 659 (2020).
<https://doi.org/10.3103/S0967091220100095>
18. G. V. Shishalova, M. A. Kulakova, and E. E. Varlashova, *Analitika i kontrol* **7** (2), 186 (2003) [in Russian].
19. A. A. Pupyshev and D. A. Danilova, *Analitika i kontrol* **11** (2–3), 131 (2007) [in Russian].

Translated by V. Isaakyan

Publisher's Note. Pleiades Publishing remains neutral with regard to jurisdictional claims in published maps and institutional affiliations.